

UNIVERSITY
OF MIAMI



High Latitude Sea Surface Skin Temperatures Derived From Saildrone Infrared Measurements

Rosenstiel School of Marine and Atmospheric Science
University of Miami

Presenter: Chong Jia

ORCID: <https://orcid.org/0000-0002-6641-5589>

Co-authors: Peter Minnett, Malgorzata Szczodrak, Miguel Izaguirre



Content

1. Introduction

2. Methodology

3. Results and Analysis

4. Summary

UNIVERSITY
OF MIAMI



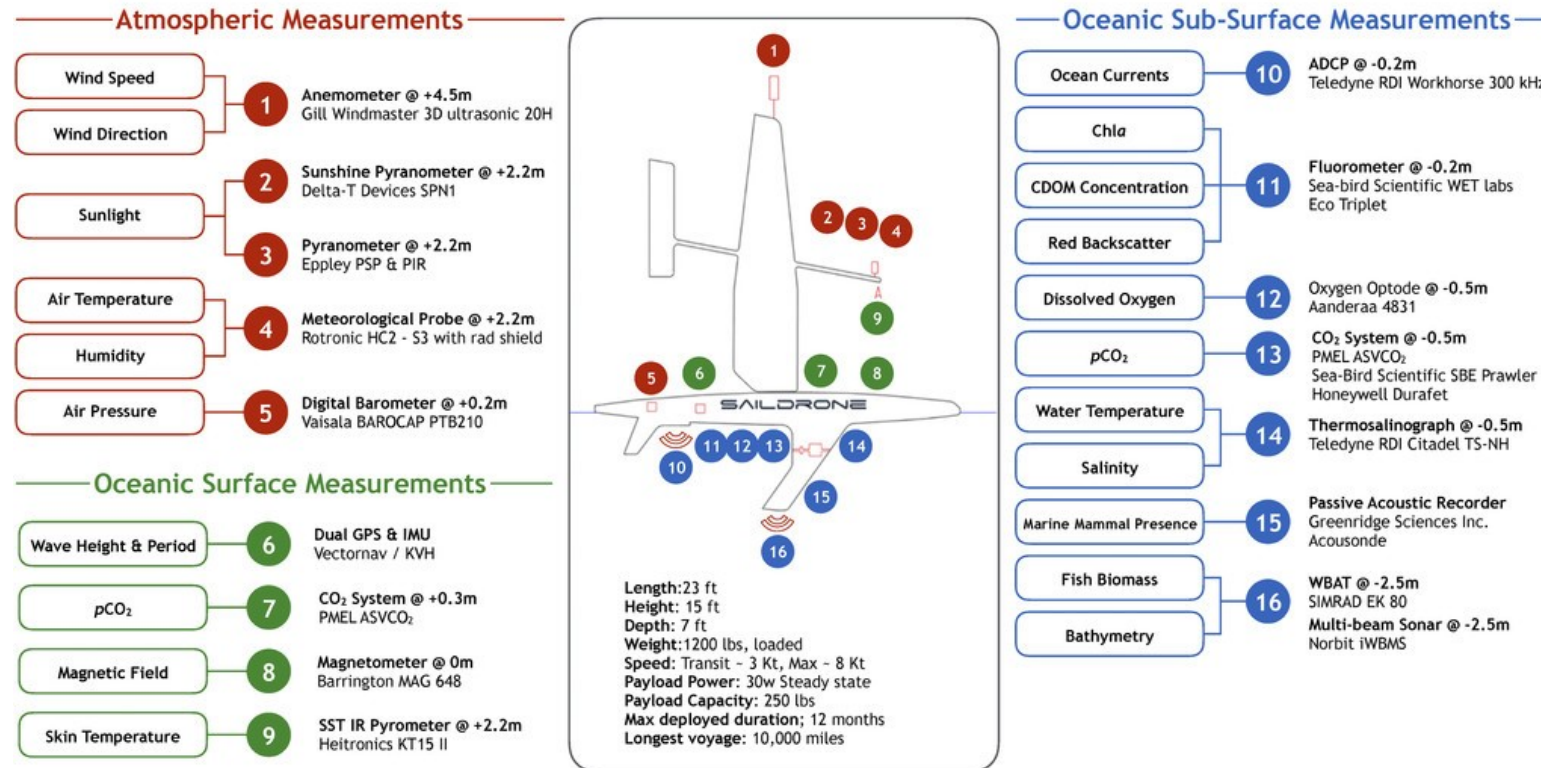
Introduction: Background

- **Infrared (IR) satellite remote sensing can provide frequent, long-term, global coverage of the sea surface skin temperature (skin SST).**
- **IR radiometers mounted on ships or other platforms have been recognized as providing appropriate, accurate skin SSTs for the satellite data validation.**
- **There are several ship-borne IR radiometer systems that have been proven to be successful in collecting skin SSTs, such as the SISTeR, the M-AERI, and the ISAR.**
- **The amount of available skin SST data is still limited in number and coverage, especially at high latitudes.**
- **Here we introduce a simple system with two IR radiation pyrometers carried on Saildrone uncrewed surface vehicles (USVs) deployed in 2019 Arctic Cruise.**



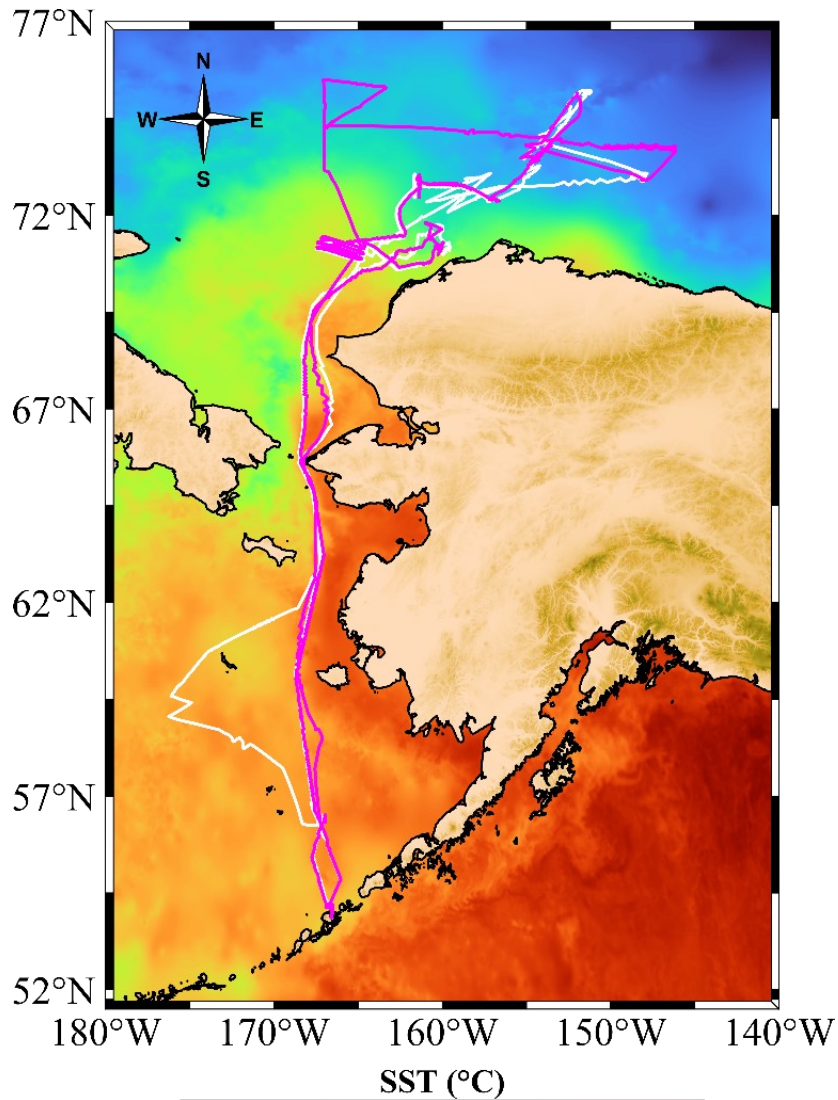
Introduction: Sailable USV

SAILDRONE GEN 4 SPECIFICATIONS AND SENSOR SUITE

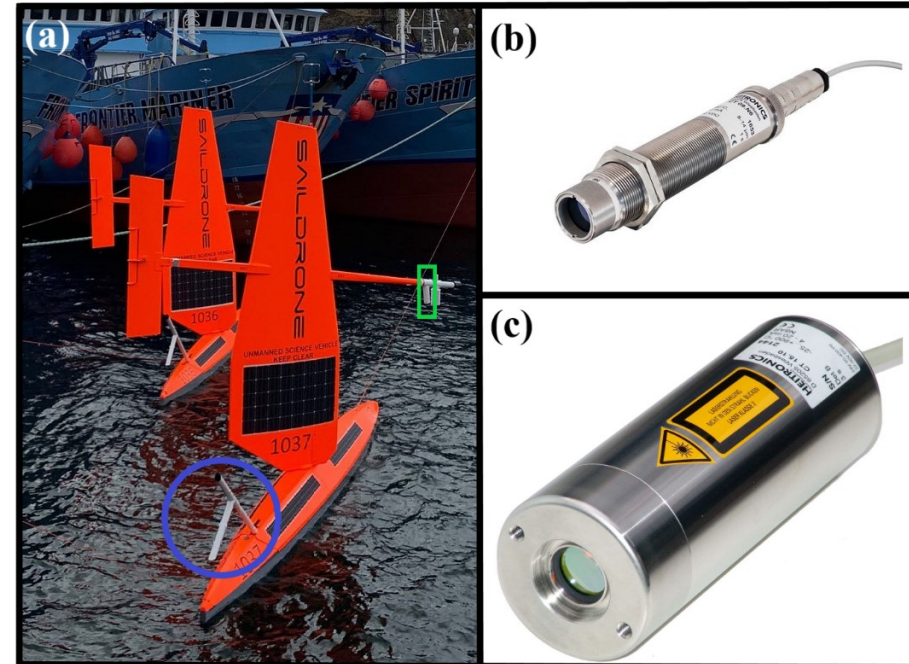


- **Wind-power for propulsion with a suite of solar-powered meteorological and oceanographic instruments.**
- **Deliver data in real time via satellite transmissions to ground stations.**

Introduction: 2019 Arctic Cruise (15 May to 11 October)



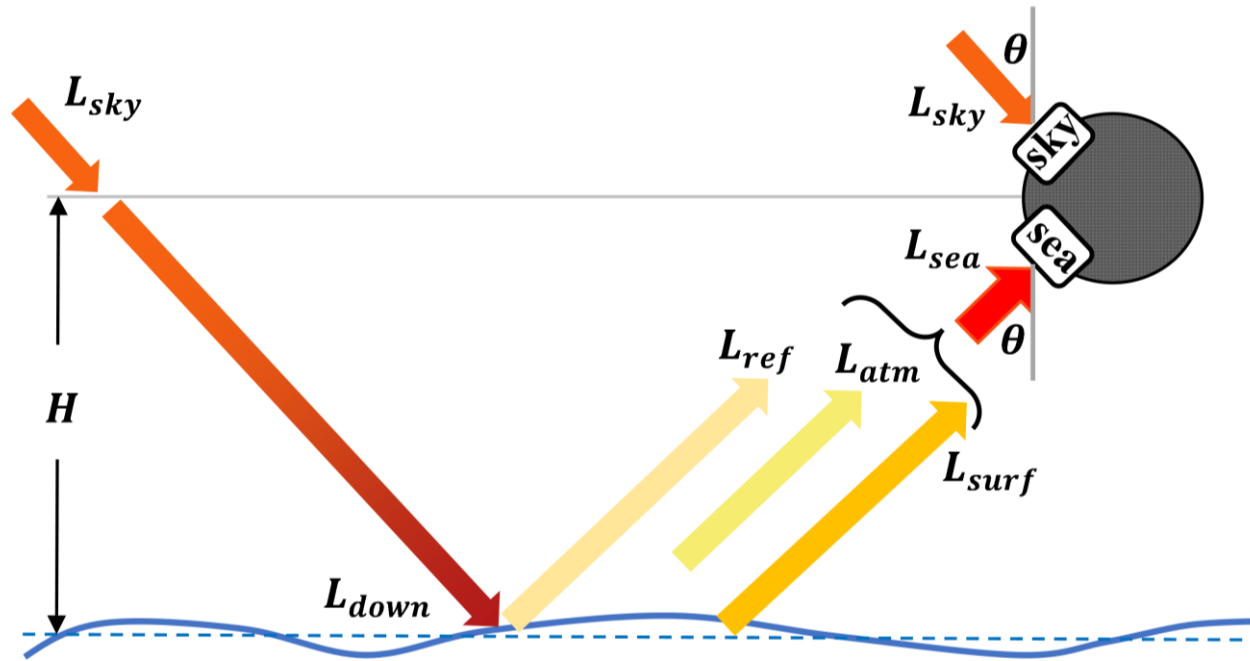
- Tracks for SD-1036 (white) and SD-1037 (magenta).
- Background SSTs are the MUR Level 4 data on 16 Sep 2019.



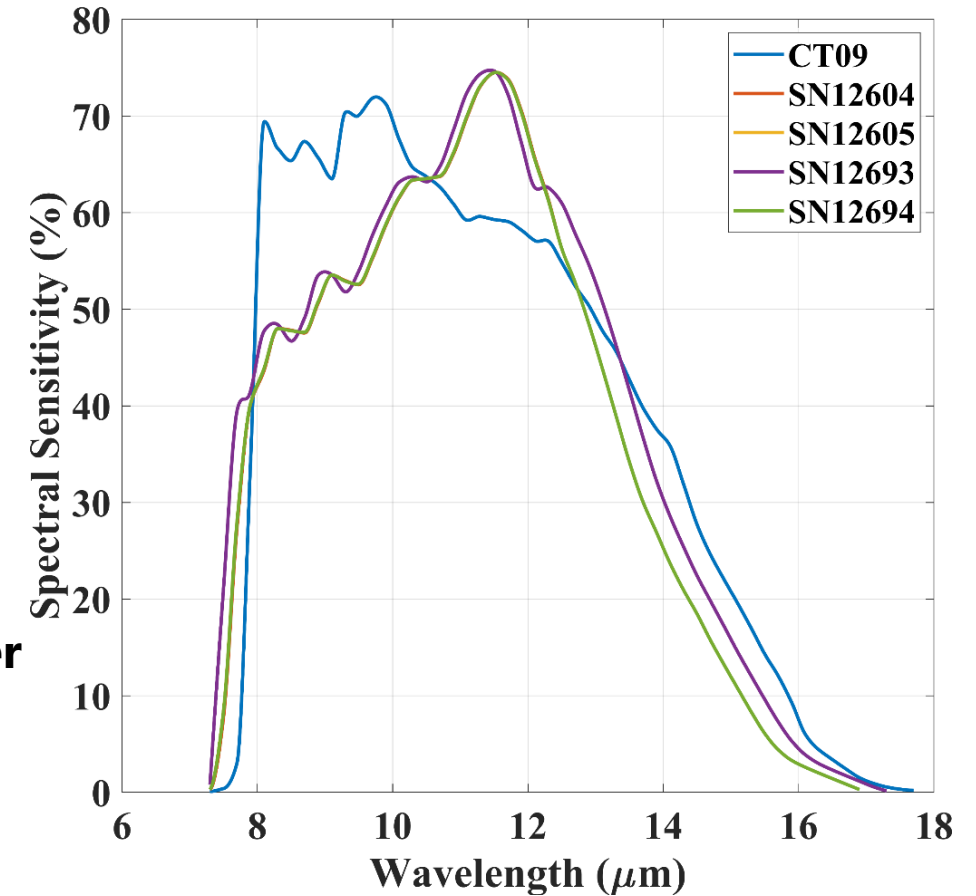
- A pair of IR pyrometers were near the bow on the deck at 0.8 m high (a; blue circle). An additional pyrometer was mounted on the spar of the sail at 2.25 m above the ocean surface (a; green box).
- Two sea-viewing sensors were CT15.10 (c), while the sky-viewing sensor was a CT09 (b).



Methodology: Saildrone Skin SST Derivation



Relative spectral response (RSR) function



Assume atmospheric transmittance from surface to radiometer of unity and consider the sea surface emissivity effect:

$$B(T_{sea}, \lambda) \approx \varepsilon(\lambda, \theta)B(T_s, \lambda) + (1 - \varepsilon(\lambda, \theta))B(T_{sky}, \lambda) \quad (1)$$

Consider the spectral response function:

$$\int_{\lambda_0}^{\lambda_1} \sigma(\lambda)B(T_{sea}, \lambda) d\lambda = \int_{\lambda_0}^{\lambda_1} \sigma(\lambda)[\varepsilon(\lambda, \theta)B(T_s, \lambda) + (1 - \varepsilon(\lambda, \theta))B(T_{sky}, \lambda)] d\lambda \quad (2)$$

Methodology: Viewing Geometry Determination

To determine the sea surface emissivity, we should determine the viewing geometry first.

Establish the three-dimensional rotation matrix:

$$R = \begin{bmatrix} \cos \gamma & -\sin \gamma & 0 \\ \sin \gamma & \cos \gamma & 0 \\ 0 & 0 & 1 \end{bmatrix} \begin{bmatrix} \cos \beta & 0 & \sin \beta \\ 0 & 1 & 0 \\ -\sin \beta & 0 & \cos \beta \end{bmatrix} \begin{bmatrix} 1 & 0 & 0 \\ 0 & \cos \alpha & -\sin \alpha \\ 0 & \sin \alpha & \cos \alpha \end{bmatrix} R' \quad (1)$$

where γ is the angle rotating about the z-axis, the yaw angle; β is the angle rotating about the y-axis, the pitch angle; α is the angle rotating about the x-axis, the roll angle.

The unit vector with reference to the IR pyrometer itself:

$$R' = \begin{bmatrix} \cos \theta_0 & 0 & \sin \theta_0 \\ 0 & 1 & 0 \\ -\sin \theta_0 & 0 & \cos \theta_0 \end{bmatrix} \begin{bmatrix} 0 \\ 0 \\ 1 \end{bmatrix} \quad (2)$$

For the sensors mounted on the hull, θ_0 is -50° (down-looking) or 50° (up-looking); for the one at the spar of wing, θ_0 is -7° .

where θ_0 is the standard viewing angle of the sensors for an upright Sairdrone.

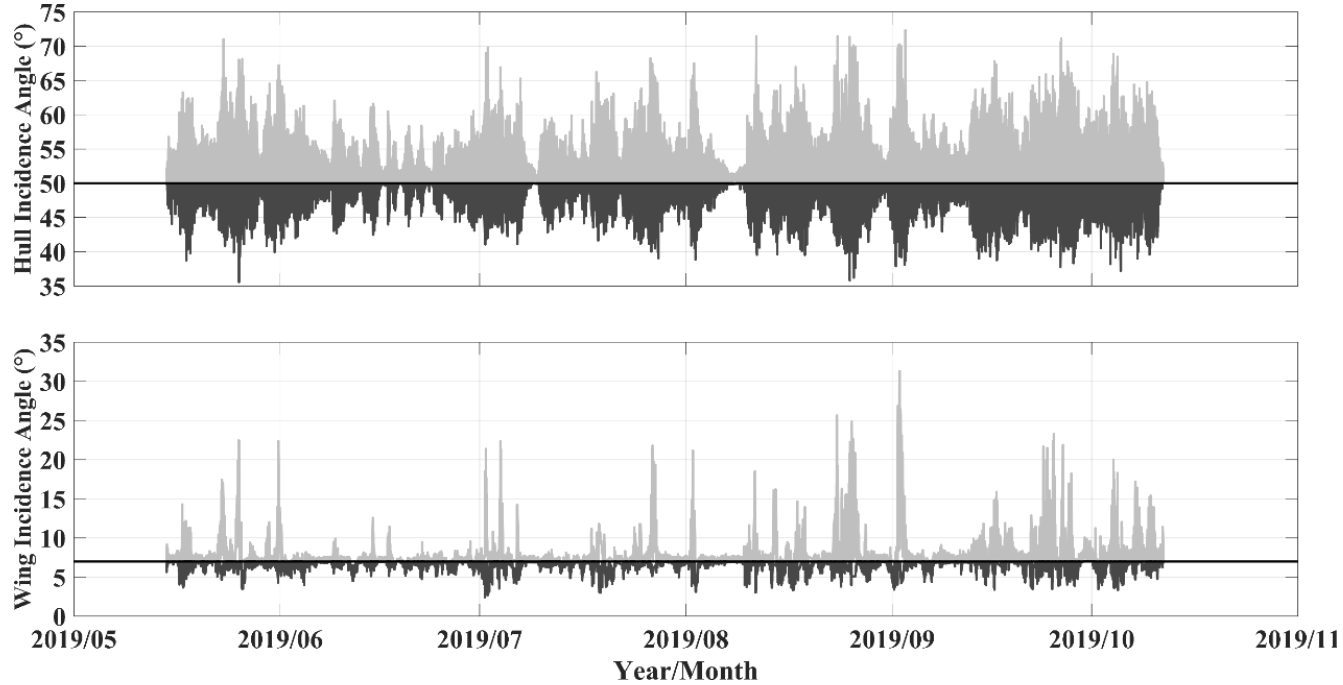
The effective incidence angle:

$$\theta_e = \arccos\left(R \cdot \begin{bmatrix} 0 \\ 0 \\ 1 \end{bmatrix}\right) \quad (3)$$



Methodology: Emissivity Calculation

Down-looking sensors on the hull and wing:

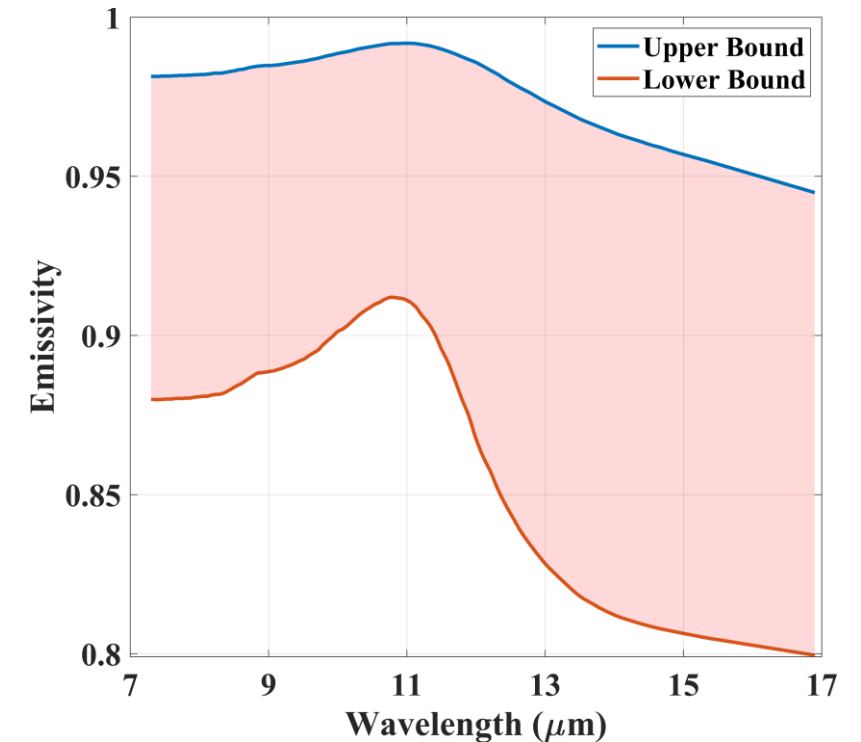


Before deriving the skin SST:

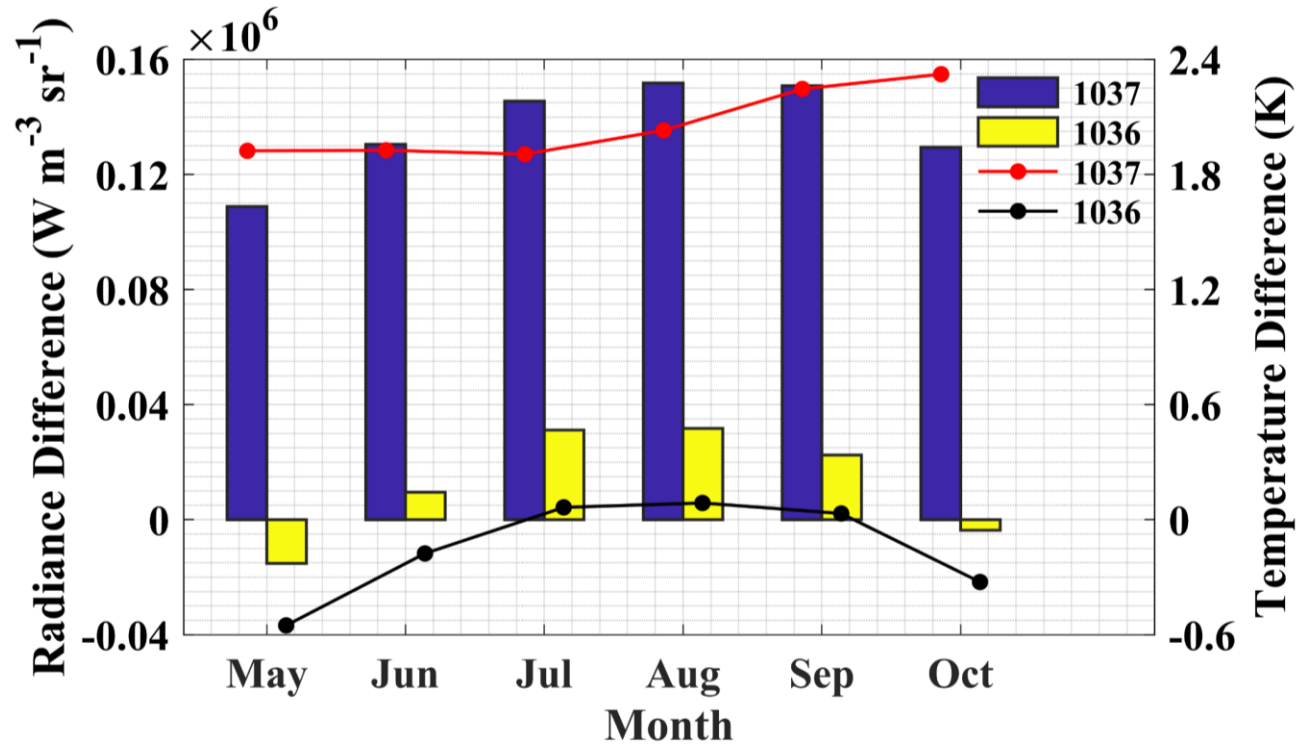
- Different RSR functions
 - Different viewing angles
- } between CT15 and CT09

Resulting in inaccuracies of using the T_{sky} for the reflected sky radiance correction

A built-in IR sea surface emissivity model (IREMIS) in RTTOV (Radiative Transfer for TOVS) model is used to determine the emissivity. This model includes the zenith angle and wind speed dependence, also the refractive indices depending on skin temperature in the 10-12 μm window.



Methodology: Numerical Simulations — RSR Functions

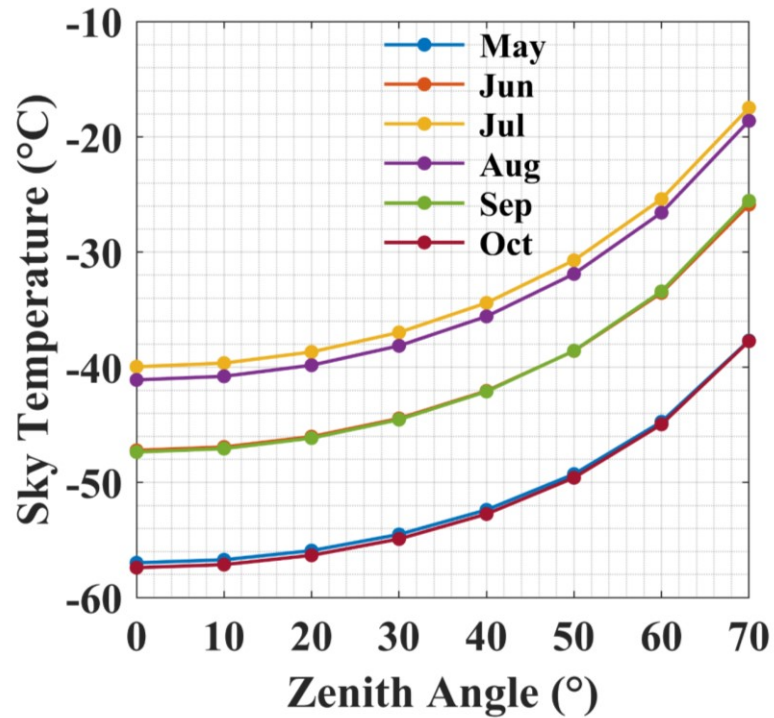


- Use the Line-By-Line Radiative Transfer Model (LBLRTM) to simulate the clear sky atmospheric downwelling radiance spectra at the surface.
- Then the radiance (and brightness temperature) measured by the IR pyrometers can be simulated based on the their RSR functions.
- MERRA-2 data, as model inputs for meteorological fields, have been averaged by month in the target area ($50^{\circ}\text{N}\sim 75^{\circ}\text{N}$, $180^{\circ}\text{W}\sim 140^{\circ}\text{W}$) with land mask.

- The simulations of the sky radiance (bars) and corresponding temperature (dots and lines) differences measured by CT15 and CT09 at a zenith angle of 50° from May to October 2019.
- For SD-1036, CT09 would generally measure the T_{sky} 0.15 K (ignore) warmer than that would have been measured by CT15 under clear skies, whereas for SD-1037, it reaches up to 2 K colder on average, causing 0.025 K error in skin SST.

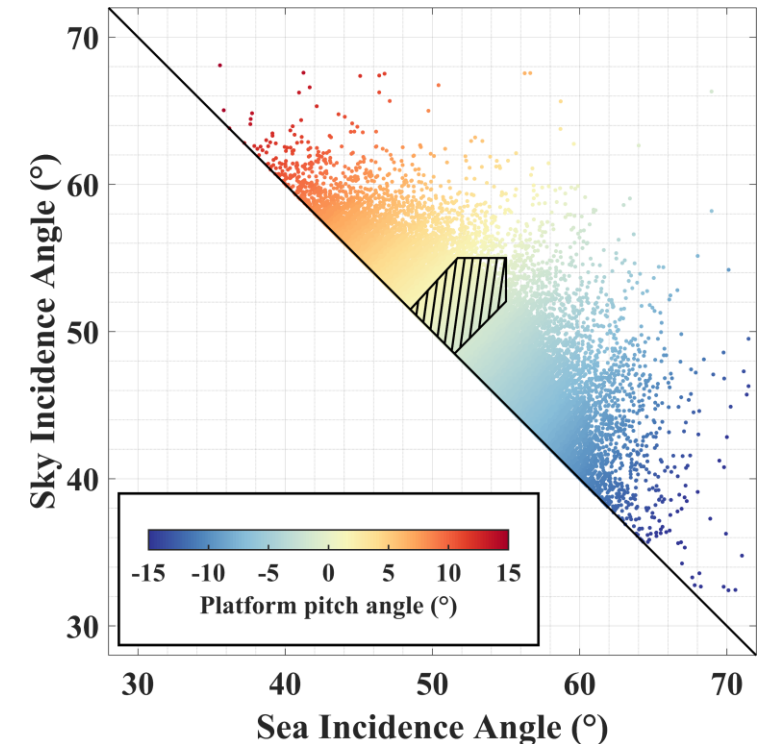


Methodology: Numerical Simulations — Viewing Angles



- To further examine the effects of inconsistent sea- and sky-viewing angles due to the pitching of Saildrone, the input zenith angle was set from 0 to 70° in increments of 10° based on the LBLRTM simulation mentioned above.
- Both the ranges of the sea- and sky-viewing angles to be used are limited within 45° to 55°. Furthermore, the platform pitch angles are also limited within $\pm 1.5^\circ$.

- Due to those limitations (shadow area), the angle discrepancies have been finally controlled within $\pm 3^\circ$, and the resulting T_{sky} uncertainties are $< \pm 1.5$ K, which introduces a maximum error in the derived skin SST < 0.02 K under clear sky conditions.

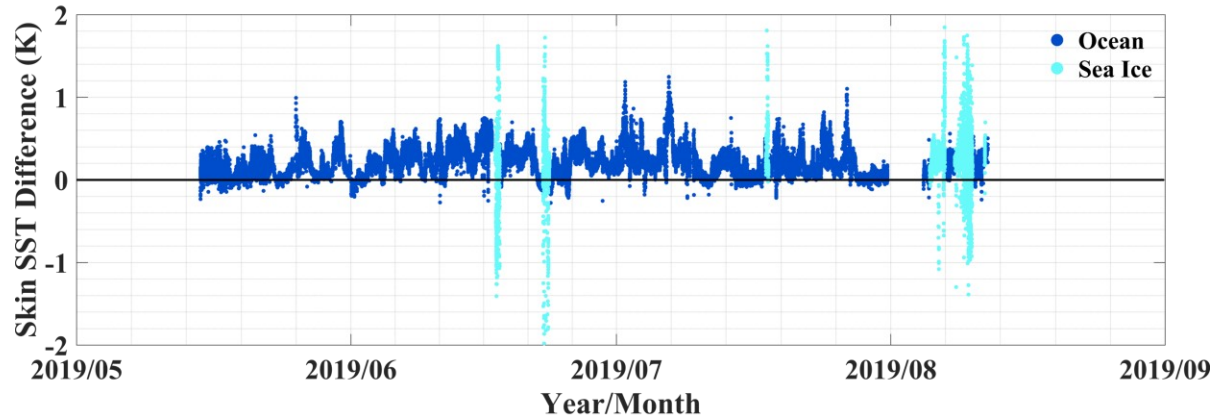


Results and Analysis: Hull and Wing Skin SSTs

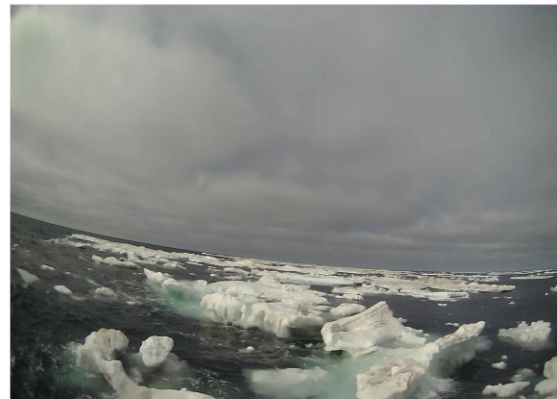
Derive skin SST:

$$\int_{\lambda_0}^{\lambda_1} \sigma(\lambda) B(T_{sea}, \lambda) d\lambda = \int_{\lambda_0}^{\lambda_1} \sigma(\lambda) [\varepsilon(\lambda, \theta) B(T_s, \lambda) + (1 - \varepsilon(\lambda, \theta)) B(T_{sky}, \lambda)] d\lambda$$

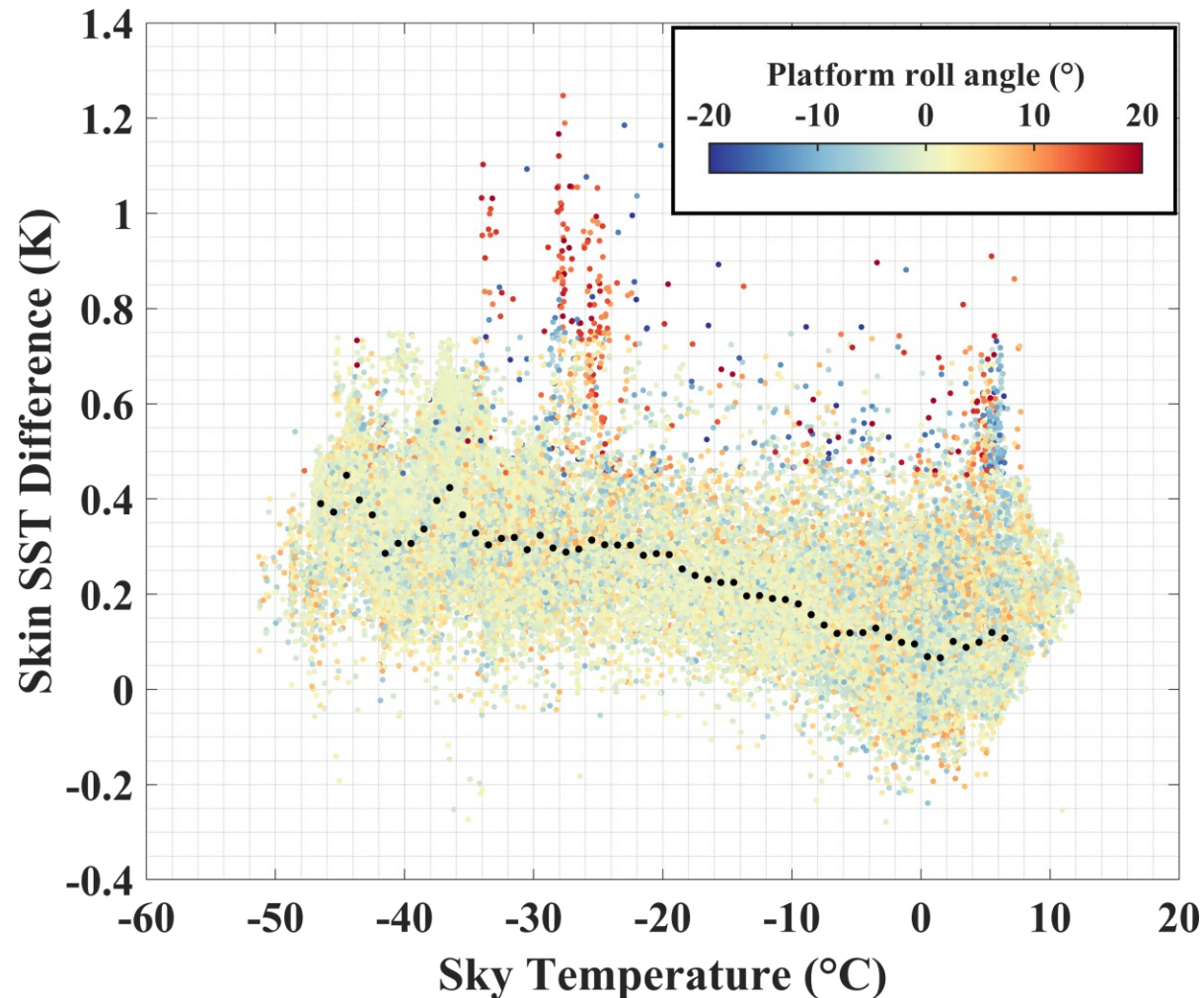
Compare skin SST from hull and wing:



- The single radiometer installed on the wing had no matched sky-viewing sensor.
- Some large positive and negative differences are distinct at certain periods, which could be identified in images recorded by the cameras onboard as sea ice contamination.
- Removing those measurements, the hull SSTs are generally warmer than wing SSTs. This is mainly due to the inappropriate warmer T_{sky} used for correcting the wing data.



Results and Analysis: Hull and Wing Skin SSTs



- The hull and wing SST differences have a dependence on T_{sky} .
- Rain droplets on the surface of the lens can give rise to the measured T_{sky} with a warm bias due to the higher temperature of raindrops, resulting in hull SST < wing SST.
- The large differences are mainly characterized by the large roll angles of platform, leading to T_{sky} with more significant warm bias for the wing SST derivation.



Error Budget Analysis (Hull SST)

Three main components of inaccuracy:

- Sea surface emissivity (assume to be very small)
- Sky-viewing radiometer measurement (**instrument, viewing angle and RSR function**)
- Sea-viewing radiometer measurement (**instrument**)

$$\epsilon_{skin}^2 = \epsilon_{sea}^2 + \epsilon_{sky}^2 + \epsilon_{angle}^2 + \epsilon_{RSR}^2$$

	CT09 (Sky)	CT15 (Sea)
Manufacturer's stated accuracy	± 1.0 K plus 0.6% of the difference between target and instrument temperature	± 0.5 K plus 0.7% of the difference between target and instrument temperature

- The total error from the last three terms is no more than 0.024 K for SD-1036 and 0.036 K for SD-1037.
- The accuracy of CT15 (0.5 K) given in the manufacturer's specifications is not acceptable.



Error Budget Analysis (Hull SST)

To evaluate the skin SST uncertainty, compare skin SST difference with the subsurface SST difference measured by Sea-Bird SBE 56 temperature loggers at 0.3 m between SD-1036 and SD-1037 within small separations (10 km).

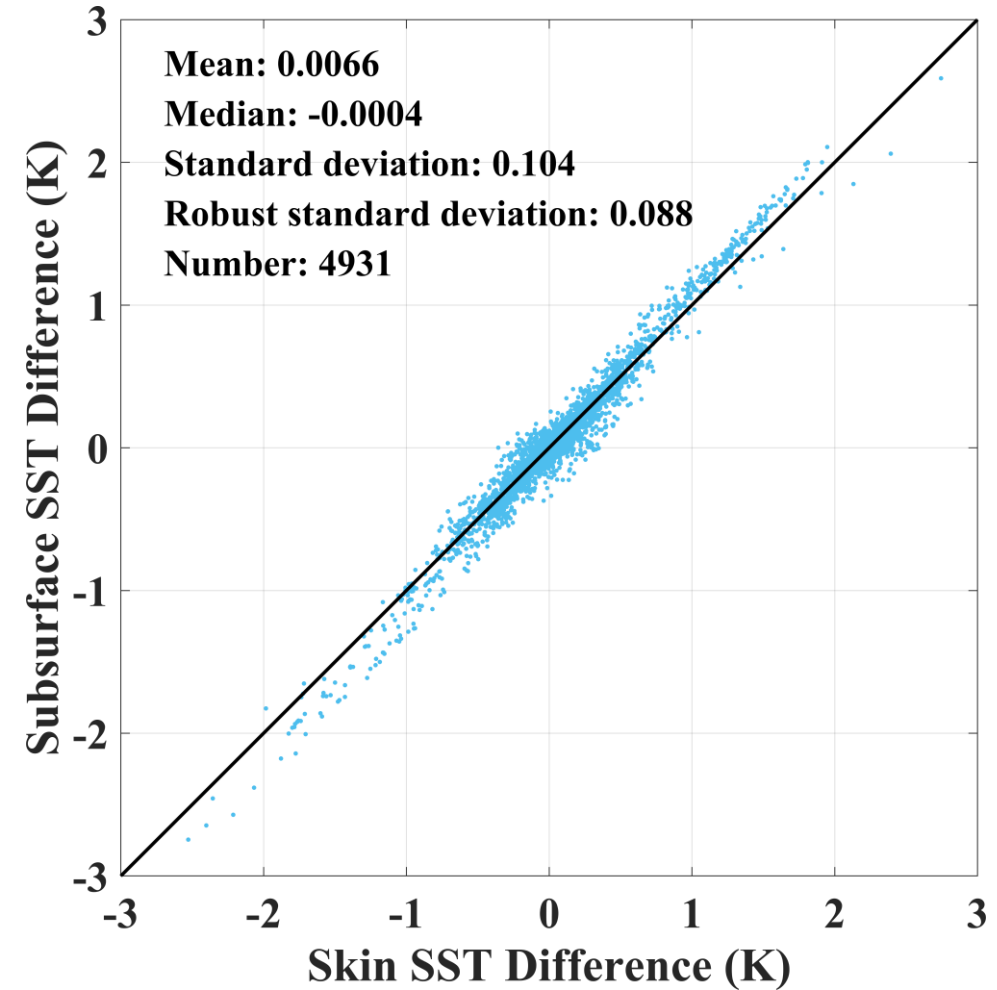
$$\Delta\text{SST}_{\text{skin}} = \text{SST}_{\text{skin}_{1036}} - \text{SST}_{\text{skin}_{1037}} = u_c + \delta(\text{SST}_{\text{skin}}) \quad (1)$$

$$\Delta\text{SST}_{0.3 \text{ m}} = \text{SST}_{0.3 \text{ m}_{1036}} - \text{SST}_{0.3 \text{ m}_{1037}} = \delta(\text{SST}_{0.3 \text{ m}}) \quad (2)$$

$$\delta(\text{SST}_{\text{skin}}) = \delta(\text{SST}_{0.3 \text{ m}}) \quad \text{Remove diurnal heating signals} \quad (3)$$

$$u_c = \sqrt{u_{1036}^2 + u_{1037}^2} = 1.96 * \text{RSD}(\Delta\text{SST}_{\text{skin}} - \Delta\text{SST}_{0.3 \text{ m}}) \quad (4)$$

$$u_{\text{SST}_{\text{skin}}} = u_{1036} = u_{1037} = 0.12 \text{ K} \quad (5)$$



Summary

- **To obtain sufficiently accurate emissivity for skin SST derivations, the viewing geometry of sensors must be well established given the effects of the vehicle's pitching and rolling.**
- **The skin SSTs are highly likely to be contaminated when the Saildrones were close to or stuck in the sea ice, and also in, and for some time after, rainfall.**
- **The errors of skin SST retrievals mainly come from the inaccuracies of both measured sea and sky radiometric temperatures and largest component is instrumental uncertainty in the sea-viewing CT15 measurements.**
- **The instrumental uncertainty of CT15 is much smaller than 0.5 K given in the manufacturer's specifications. The skin SSTs derived from the infrared pyrometers mounted on the hull of Saildrones have an estimated uncertainty of 0.12 K, which is sufficiently accurate to be used in many scientific studies.**



UNIVERSITY
OF MIAMI



Thank You !

**Funding acknowledgement: University of Miami Graduate Fellowship
and NASA through the Oceanographic Partnership Program (NOPP)**

